Distributed observer-based leader-following consensus control for LPV multi-agent systems: Application to multiple VTOL-UAVs formation control

Jesus A. Vazquez Trejo, Jean-Christophe Ponsart, Manuel Adam-Medina, Guillermo Valencia-Palomo, Didier Theilliol

Distributed Observer-based Leader-following Consensus Control for LPV Multi-agent Systems: Application to multiple VTOL-UAVs Formation Control

Jesus A. Vazquez Trejo[1,2], Jean-Christophe Ponsart[1], Manuel Adam-Medina[2], Guillermo Valencia-Palomo[3] and Didier Theilliol[1]

***Abstract*— This paper presents a distributed observer-based leader-following consensus control for linear parameter-varying multi-agent systems. The stability of the observer and the controller is proved by the Lyapunov theory. It is shown that the design conditions of the estimated states and consensus control are expressed in a set of linear matrix inequalities considering Polya's theorem for less conservatism. To show the effectiveness of the proposed strategy, the formation control problem on a team of vertical take-off and landing unmanned aerial vehicles are considered in the simulation results.**

I. INTRODUCTION

In the last decades, Multi-Agent Systems (MASs) have been of interest due to their potential compared with the performance of a single agent [1], where an agent is defined as an autonomous dynamical system. The control problem is to design an appropriate controller to coordinate every agent to achieve a global objective [2]. Different strategies to coordinate MASs can be considered, such as: *consensus-based* [3], which objective is that agents converge to a common value by interacting with each other via a communication network; *Leader-following* [4], where the agents are considered followers of another agent, which can be a real system or a virtual system, this agent is a reference for the others and is commonly known as a leader; *Virtual structure strategies* [5] consider that the agents have geometric relations between them and with a reference frame, this is a leaderless method, but the stability of the MASs is not guaranteed; *Behavior-based strategies* [6] are biological techniques inspired by the joint movement of some animals in nature, it is assumed that the agents are able to obtain information from their environment and communicate with each other to generate a global grouping behavior; *Artificial potentials* [7], where agents are assumed to be able to avoid collisions, consider dynamic distances between agents, or track trajectories and targets; *graph-theory strategies* [8] are commonly used to model the communications between agents and guarantee the stability of the MASs. The coordination of MASs is essential to accomplish common objectives [9], some of these objectives are formation control [10], formation tracking [11], and leader-following UAV swarms [12], among others.

Recently, the use of Unmanned Aerial Vehicles (UAVs) has become promising mobile platforms capable of autonomous navigation. An extensive number of applications of UAVs have been proposed, such as agriculture assessment [13], search and rescue missions [14], marine exploration [15], and fire monitoring [16], among others [17]. Research works based on MASs using UAVs have considered the leader-following consensus related to Linear Time-Invariant (LTI) focused on second-order MASs with irregular discrete sampling times [18], particle swarm optimization [19], event-triggered mechanisms [20], and communication faults [21]. Furthermore, [22] proposed an observer-based consensus control against actuator faults for Linear Parameter-Varying (LPV) MASs. Moreover, a gain-scheduled observer-based consensus for LPV MASs is investigated in [23], where the controller and observer gains are functions of some time-varying parameter vector that is measured in real-time, Polya's theorem [24] is considered to reduce conservatism compared with the work of [22].

The main contribution of this paper is the design of a leader-following consensus control for MASs. Linear Matrix Inequalities (LMIs) conditions are obtained to guarantee the existence of the polytopic controller and observer gains for a team of LPV MASs based on leader-following consensus control observer-based inspired by the work of [22] and [23]. The main differences from previous works are the leader-following consensus for MASs, the use of the Schur complement [25] and the Young relation [26] to determine the LMIs conditions considering Polya's theorem. In order to validate the proposal, the developed strategy is applied to a team of nonlinear quadcopters where the solution for the LMIs is computed using the quasi-LPV representation of the UAVs.

This paper is organized as follows. The problem statement and system description are presented in Section II. In Section III, the proposed LPV observer-based leader-following control is designed. The quasi-LPV representation of the nonlinear quadcopter model is presented in Section IV. The simulation results to show the effectiveness of this approach are presented in Section V. The conclusions are shown in Section VI.

[1] University of Lorraine, CRAN, UMR 7039 CNRS, Nancy, France jesus-avelino.vazquez-trejo@univ-lorraine.fr Jean-christophe.Ponsart@univ-lorraine.fr didier.theilliol@univ-lorraine.fr

[2]TecNM/CENIDET, Electronic engineering department, Cuernavaca, Morelos 62490, Mexico manuel.am@cenidet.tecnm.mx

[3]TecNM/Hermosillo, Av. Tec y Per Poniente S/N, 83170, Hermosillo, Mexico. gvalencia@hermosillo.tecnm.mx

Consider for the Best Student Paper Award

PRELIMINARIES

Notation. To simplify the notation, the symbol $*$ represents the symmetric elements of a matrix. The Kronecker product is denoted by the symbol $\otimes$. The Hermitian part of a square matrix $\mathcal{Z}$ is denoted by $\text{He}\{\mathcal{Z}\} = \mathcal{Z} + \mathcal{Z}^T$. Given $s \in \mathbb{N}$, the symbol $\mathbb{D}_s$ and $\mathbb{D}_s^+$ denote the following sets:

$$\mathbb{D}_s = \left\{ \vec{d} = \left[\vec{d}_1, \ldots, \vec{d}_s\right]^T \in \mathbb{N}^s | 1 \leq \vec{d}_k \leq s \, \forall k = 1, \ldots, s \right\}, \tag{1}$$

$$\mathbb{D}_s^+ = \left\{ \vec{d} \in \mathbb{D}_s | \vec{d}_k \leq \vec{d}_{k+1}, k = 1, \ldots, s-1 \right\}, \tag{2}$$

where the set of permutations with possible repeated elements of the multi-index $\vec{d}$ is denoted by $\mathcal{D}(\vec{d}) \subset \mathbb{D}_s$.

II. PROBLEM STATEMENT

Let us consider the following LPV multi-agent system

$$\begin{aligned} \dot{x}_i(t) &= A(\zeta_i(t))x_i(t) + B(\zeta_i(t))u_i(t), \\ y_i(t) &= C(\zeta_i(t))x_i(t), \end{aligned} \tag{3}$$

composed of N identical systems. For each one, i is the agent number ($i = 1, \ldots, N$); $x_i(t) \in \mathbb{R}^n$, $u_i(t) \in \mathbb{R}^r$, $y_i(t) \in \mathbb{R}^p$, are the state, input, and output, vectors respectively; $A(\zeta_i(t)) \in \mathbb{R}^{n \times n}$, $B(\zeta_i(t)) \in \mathbb{R}^{n \times r}$, and $C(\zeta_i(t)) \in \mathbb{R}^{p \times n}$ are the matrix functions scheduled by the vector $\zeta_i(t) \in \mathbb{R}^{n_\zeta}$, which is considered known and available for every i-th agent, and is assumed to vary in a closed set $\mathcal{R}$. The *bounding box* method [27] is used in order to express $A(\zeta_i(t)), B(\zeta_i(t))$, and $C(\zeta_i(t))$ as a convex combination of S vertex matrices, such that

$$\begin{aligned} &\begin{pmatrix} A(\zeta_i(t)) \\ B(\zeta_i(t)) \\ C(\zeta_i(t)) \end{pmatrix} = \sum_{h=1}^{S} \rho_h(\zeta_i(t)) \begin{pmatrix} A_h \\ B_h \\ C_h \end{pmatrix}, \\ &\sum_{h=1}^{S} \rho_h(\zeta_i(t)) = 1, \quad \rho_h(\zeta_i(t)) \geq 0 \quad \forall \zeta_i(t) \in \mathcal{R} \end{aligned} \tag{4}$$

where each agent is considered as an autonomous dynamical system able to share the information of their states with the neighboring agents. Then, in order to design the communication exchange between agents, some elements of graph theory are recalled.

Let consider a directed graph $\mathcal{G}(\mathcal{V}, \mathcal{E}, \mathcal{A})$ where $\mathcal{V} = \{v_1, v_2, \ldots, v_N\}$ is a set of nodes (agents), $\mathcal{E} = \{(i,j) : i, j \in \mathcal{V}\} \subseteq \mathcal{V} \times \mathcal{V}$ is a set of edges, and the adjacency matrix $\mathcal{A} = [a_{ij}] \in \mathbb{R}^{N \times N}$ is defined as $a_{ii} = 0$, $a_{ij} > 0$ if and only if the pair $(i,j) \in \mathcal{E}$, otherwise $a_{ij} = 0$. When the graph is undirected, also, $a_{ij} = a_{ji}$, $\forall i \neq j$ and $\mathcal{A} = \mathcal{A}^T$. The Laplacian matrix $\mathcal{L} \in \mathbb{R}^{N \times N}$ is defined as $\mathcal{L}_{ii} = \sum_{j \neq i} a_{ij}$ and $\mathcal{L}_{ij} = -a_{ij}$. The set of neighbors related to the i-th agent is denoted as $j \in \mathcal{N}_i$. α_i is related with the leader, $\alpha_i = 1$ if there is a link between the i-th agent and the leader, otherwise $\alpha_i = 0$. The following assumptions are held in this work ($\forall h = 1, \ldots, S$):

Assumption 1: The pair (A_h, B_h) is stabilizable.

Assumption 2: The pair (A_h, C_h) is observable.

Assumption 3: The graph $\mathcal{G}$ is undirected.

The main objective of this work is the design of a leader-following control for LPV multi-agent systems consensus-based. The LPV virtual leader dynamic is defined by:

$$\dot{x}_l(t) = A(\zeta_l(t))x_l(t) + B(\zeta_l(t))u_l(t), \tag{5}$$

where $x_l(t) \in \mathbb{R}^n$, $u_l(t) \in \mathbb{R}^r$ are the state and input vectors of the virtual leader. Consensus between the leader and the followers can be achieved only if $\zeta_1(t) = \zeta_2(t) = , \ldots, = \zeta_N(t) = \zeta_l(t) = \zeta(t)$. Let $\delta_i(t) = x_i(t) - x_l(t)$, then, the dynamics of the synchronization error between each agent i and the leader is:

$$\dot{\delta}_i(t) = A(\zeta(t))\delta_i(t) + B(\zeta(t))\big(u_i(t) - u_l(t)\big). \tag{6}$$

Let us propose the following observer-based consensus protocol:

$$\begin{aligned} u_i(t) = K(\zeta(t)) \Bigg[\sum_{j \in \mathcal{N}_i} \big(\hat{x}_i(t) - \hat{x}_j(t)\big) + \\ \alpha_i \big(\hat{x}_i(t) - x_l(t)\big) \Bigg] + u_l(t), \end{aligned} \tag{7}$$

where $K(\zeta(t)) \in \mathbb{R}^{r \times n}$ is the LPV control gain to be designed and $\hat{x}_j(t) \in \mathbb{R}^n$ are the estimated states of the neighboring agents. Due to the estimated states of agent i and agent j are considered in the consensus protocol (7), the estimated state vector $\hat{x}_i(t) \in \mathbb{R}^n$ is given by the following distributed LPV observer:

$$\begin{aligned} \dot{\hat{x}}_i(t) &= A(\zeta(t))\hat{x}_i(t) + B(\zeta(t))u_i(t) \\ &\quad + L(\zeta(t))\Big(y_i(t) - \hat{y}_i(t)\Big), \\ \hat{y}_i(t) &= C(\zeta(t))\hat{x}_i(t), \end{aligned} \tag{8}$$

where $L(\zeta(t)) \in \mathbb{R}^{n \times p}$ is the LPV observer gain to be designed and $\hat{y}_i(t) \in \mathbb{R}^p$ is the estimated output vector. The polytopic representation of the control gain $K(\zeta(t))$ and the observer gain $L(\zeta(t))$ are considered as follows:

$$\begin{pmatrix} K(\zeta(t)) \\ L(\zeta(t)) \end{pmatrix} = \sum_{h=1}^{S} \rho_h(\zeta(t)) \begin{pmatrix} K_h \\ L_h \end{pmatrix}. \tag{9}$$

Defining the estimation error $e_i(t) = x_i(t) - \hat{x}_i(t)$, then, the dynamics of the estimation error are:

$$\dot{e}_i(t) = A(\zeta(t)) - L(\zeta(t))C(\zeta(t)))e_i(t). \tag{10}$$

The design of the vertex control gains K_h and the vertex observer gains L_h using LMIs and computed simultaneously, is the main problem.

III. LPV OBSERVER-BASED LEADER-FOLLOWING CONSENSUS CONTROLLER

The LMI conditions to guarantee the existence of the control and observer gains are presented in this section using the Lyapunov stability analysis. Let us consider the time-varying parameters vector $\zeta(t) = [\zeta_1(t)^T, \zeta_2(t)^T, \ldots, \zeta_N(t)^T]^T$, defining the matrix:

$$\rho_{ij}(\zeta(t)) = diag(\rho_{i \star j}(\zeta_1(t)), \ldots, \rho_{i \star j}(\zeta_N(t))) \tag{11}$$

with $\rho_{i\star j}(\zeta_g(t)) \triangleq \rho_i(\zeta_g(t))\rho_j(\zeta_g(t))$, $g = 1, \ldots, N$. Considering $e(t) = [e_1(t)^T, e_2(t)^T, \ldots, e_N(t)^T]^T$, and $\delta(t) = [\delta_1(t)^T, \delta_2(t)^T, \ldots, \delta_N(t)^T]^T$, the estimation error and the synchronization error are expressed using the Kronecker product as follows:

$$\dot{e}(t) = \sum_{h=1}^{S}\sum_{g=1}^{S} \left[\rho_{hg}(\zeta(t)) \otimes (A_h - L_h C_g)\right] e(t), \tag{12}$$

$$\begin{aligned}\dot{\delta}(t) = \sum_{h=1}^{S}\sum_{g=1}^{S} \rho_{hg}(\zeta(t)) \left[I_N \otimes A_h + \bar{\mathcal{L}} \otimes B_g K_h\right] \delta(t) - \\ \left[\rho_{hg}(\zeta(t))\bar{\mathcal{L}} \otimes B_g K_h\right] e(t)\end{aligned} \tag{13}$$

where $\bar{\mathcal{L}} = \mathcal{L} + \Lambda$ is the sum of the Laplacian matrix $\mathcal{L}$ and $\Lambda = diag(\alpha_1, \alpha_2, \ldots, \alpha_N)$, the communication exchange between the leader and the followers. Let $z(t) = [\delta(t)^T, e(t)^T]^T$, then the closed-loop multi-agent system is expressed as follows (for easy notation, the time dependency is removed):

$$\begin{aligned}\dot{z} = &\sum_{h=1}^{S}\sum_{g=1}^{S} \rho_h(\zeta)\rho_g(\zeta) \\ &\times \begin{bmatrix} I_N \otimes A_h + \overline{\mathcal{L}} \otimes B_g K_h & -\overline{\mathcal{L}} \otimes B_g K_h \\ 0 & I_N \otimes (A_h - L_h C_g) \end{bmatrix} z.\end{aligned} \tag{14}$$

Let us choose a quadratic candidate Lyapunov function as follows:

$$V(z) = \begin{bmatrix}\delta^T & e^T\end{bmatrix} \begin{bmatrix} I_N \otimes P_1 & 0 \\ 0 & I_N \otimes P_2 \end{bmatrix} \begin{bmatrix}\delta \\ e\end{bmatrix}. \tag{15}$$

The following theorem provides LMI-based conditions that guarantee the existence of the LPV control and LPV observer gains based on the Lyapunov stability analysis.

Theorem 1: Consider the closed-loop LPV multi-agent system (14). The estimation (12) and synchronization (13) errors are proven to be exponentially stable by (15) for any $s \in \mathbb{N}$, with $s \geq 2$, given the eigenvalues $\lambda_j(\bar{\mathcal{L}})$, $\forall j = 1, 2, \ldots, N$; if there exist symmetric matrices $\bar{P}_1 > 0 \in \mathbb{R}^{n\times n}$ and $P_2 > 0 \in \mathbb{R}^{n\times n}$, matrices $N_1, N_2, \ldots, N_S$, and $M_1, M_2, \ldots, M_S$; the tuning scalar variable $\mu > 0$, such that

$$\sum_{\vec{\varrho}\in\mathcal{D}(\vec{d})} \begin{bmatrix} \mathcal{Q}_{j_{11}} & 0 & \mathcal{Q}_{j_{13}} & 0 \\ * & \mathcal{Q}_{22} & 0 & I_N \\ * & * & -\mu^{-1}\bar{P}_1 & 0 \\ * & * & * & -\mu\bar{P}_1 \end{bmatrix} < 0 \tag{16}$$

holds $\forall \vec{d} \in \mathbb{D}_s^+$, where $\mathcal{Q}_{j_{11}} = \text{He}\{A_{\vec{\varrho}_1}\bar{P}_1 + \lambda_j B_{\vec{\varrho}_2} N_{\vec{\varrho}_1}\}$,$\mathcal{Q}_{22} = \text{He}\{P_2 A_{\vec{\varrho}_1} - M_{\vec{\varrho}_1} C_{\vec{\varrho}_2}\}$, and $\mathcal{Q}_{j_{13}} = -\lambda_j B_{\vec{\varrho}_2} N_{\vec{\varrho}_1}$, then, the control vertex gain can be computed with $K_h = N_h \bar{P}_1^{-1}$ and the observer vertex gain with $L_h = P_2^{-1} M_h$.

Proof. The derivative of (15) along the trajectories of (14) is given by:

$$\begin{aligned}\dot{V}(z) = &\sum_{h=1}^{S}\sum_{g=1}^{S} \rho_h(\zeta)\rho_g(\zeta)\Big\{2\delta^T(I_N \otimes P_1 A_h + \\ &\bar{\mathcal{L}} \otimes P_1 B_g K_h)\delta - 2\delta^T(\bar{\mathcal{L}} \otimes P_1 B_g K_h)e \\ &+ 2e^T(I_N \otimes P_2(A_h - L_h C_g))e\Big\}.\end{aligned} \tag{17}$$

Let us perform a spectral decomposition of the matrix $\bar{\mathcal{L}}$, such that $\bar{\mathcal{L}} = TJT^{-1}$ with an invertible matrix $T \in \mathbb{R}^{N\times N}$ and a diagonal matrix $J = diag(\lambda_1, \lambda_2, \ldots, \lambda_N) \in \mathbb{R}^{N\times N}$ of which $\lambda_j(\bar{\mathcal{L}})$, $j = 1, 2, \ldots, N$ are the eigenvalues of $\bar{\mathcal{L}}$. Defining the change of coordinates as $\varphi = (T^{-1} \otimes I_N)\delta$ and $\phi = (T^{-1} \otimes I_N)e$, (17) can be rewritten as:

$$\begin{aligned}\dot{V}(z) = &\sum_{h=1}^{S}\sum_{g=1}^{S} \rho_h(\zeta)\rho_g(\zeta)\Big\{\sum_{j=1}^{N} \varphi^T \text{He}\{P_1 A_h \\ &+ \lambda_j P_1 B_g K_h\}\varphi_j - 2\sum_{j=1}^{N} \varphi^T \lambda_j P_1 B_g K_h \phi_j \\ &+ \sum_{j=1}^{N} \phi^T \text{He}\{P_2 A_h - P_2 L_h C_g\}\phi_j\Big\}.\end{aligned} \tag{18}$$

Considering the vector $[\varphi_j^T, \phi_j^T]^T$, (18) can be rewritten as follows:

$$\dot{V}(z) = \sum_{h=1}^{S}\sum_{g=1}^{S} \rho_h(\zeta)\rho_g(\zeta)\left\{ \begin{bmatrix}\varphi_j^T & \phi_j^T\end{bmatrix} \mathfrak{B}_{j_{hg}} \begin{bmatrix}\varphi_j \\ \phi_j\end{bmatrix} \right\}, \tag{19}$$

$$\mathfrak{B}_{j_{hg}} = \begin{bmatrix} \text{He}\{P_1 A_h + \lambda_j P_1 B_g K_h\} & -\lambda_j P_1 B_g K_h \\ * & \text{He}\{P_2 A_h - P_2 L_h C_g\} \end{bmatrix} \tag{20}$$

which corresponds to the problem of verifying the negativity of double polytopic sums. We define $\bar{P}_1 = P_1^{-1}$

$$\beta_{j_{hg}} = \begin{bmatrix} \bar{P}_1 & 0 \\ 0 & I_N \end{bmatrix} \mathfrak{B}_{j_{hg}} \begin{bmatrix} \bar{P}_1 & 0 \\ 0 & I_N \end{bmatrix} < 0 \tag{21}$$

$$\beta_{j_{hg}} = \begin{bmatrix} \text{He}\{A_h\bar{P}_1 + \lambda_j B_g K_h \bar{P}_1\} & -\lambda_j B_g K_h \\ * & \text{He}\{P_2 A_h - P_2 L_h C_g\} \end{bmatrix} < 0, \tag{22}$$

then, (22) can be rewritten as follows:

$$\begin{bmatrix} \beta_{j_{hg_{11}}} & 0 \\ * & \beta_{j_{hg_{22}}} \end{bmatrix} + \text{He}\left\{ \begin{bmatrix} \beta_{j_{hg_{12}}} \\ 0 \end{bmatrix} \begin{bmatrix} 0 & I_N \end{bmatrix} \right\} < 0 \tag{23}$$

where $\beta_{j_{hg_{11}}} = \text{He}\{A_h\bar{P}_1 + \lambda_j B_g K_h \bar{P}_1\}$, $\beta_{j_{hg_{22}}} = \text{He}\{P_2 A_h - P_2 L_h C_g\}$, and $\beta_{j_{hg_{12}}} = -\lambda_j B_g K_h$. Applying the Young relation [26], the following inequality is obtained:

$$\begin{aligned}\begin{bmatrix} \beta_{j_{hg_{11}}} & 0 \\ * & \beta_{j_{hg_{22}}} \end{bmatrix} + \mu \begin{bmatrix} \beta_{j_{hg_{12}}} \\ 0 \end{bmatrix} \bar{P}_1 \begin{bmatrix} \beta_{j_{hg_{12}}}^T & 0 \end{bmatrix} \\ + \mu^{-1} \begin{bmatrix} 0 \\ I_N \end{bmatrix} \bar{P}_1^{-1} \begin{bmatrix} 0 & I_N \end{bmatrix} < 0\end{aligned} \tag{24}$$

where $\mu > 0$. Using the Schur complement [25], considering $N_h = K_h \bar{P}_1$, and $M_h = P_2 L_h$ and by applying the Polya's theorem on definite quadratic forms in (19) as in [23], (16) is obtained, and the proof is completed.

IV. Quadcopter quasi-LPV model

Quasi-LPV systems are LPV systems in which the varying parameters ζ are endogenous signals, related to the internal states or input signals [28]. Theorem 1 is also fulfilled for quasi-LPV systems. Multiple UAV quadcopters are considered to illustrate the proposed leader-following consensus method. In this section, the nonlinear dynamic model of one quadcopter aerial vehicle is presented [29]. Fig. 1 shows the scheme of the quadcopter representing the main forces acting on the vehicle. To obtain this dynamic model, the following assumptions are stated [30]:

Assumption 4: The quadcopter structure is rigid and symmetrical,

Assumption 5: The center of mass and the origin of the body frame O_B coincide.

The quadcopter is composed of four independent motors with four propellers that produce torques and thrusts in the direction of the propellers axis of rotation. Propellers 1 and 3 turn in the clockwise direction, while propellers 2 and 4 turn in the counterclockwise direction. From Fig. 1, $\mathcal{I} = \{O_I, p_{x_I}, p_{y_I}, p_{z_I}\}$ denotes an inertial frame, and $\mathcal{B} = \{O_B, p_{x_B}, p_{y_B}, p_{z_B}\}$ denotes a rigid frame attached to the center of mass of the vehicle.

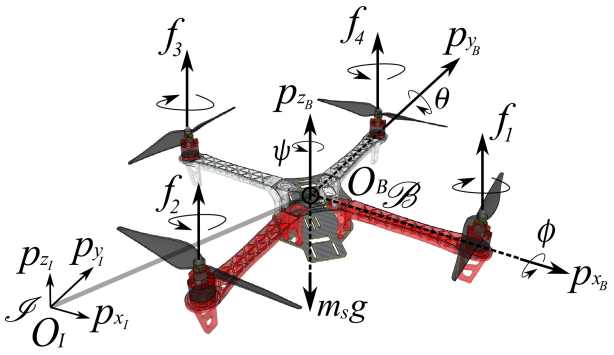

Fig. 1. Quadcopter scheme representing main forces acting in the vehicle.

The dynamics of the quadcopter can be defined as follows [31]:

$$\begin{aligned} \dot{\xi} &= v, & m_s \dot{v} &= RF, \\ \dot{R} &= R\hat{\Omega}, & J\dot{\Omega} &= -\Omega \times J\Omega + \tau, \end{aligned} \tag{25}$$

where $\xi = [p_x, p_y, p_z]^T \in \mathbb{R}^3$ and $v = [v_x, v_y, v_z]^T \in \mathbb{R}^3$ denotes the position and velocity of the vehicle with respect to the frame $\mathcal{I}$, respectively. The angular velocity is defined by $\Omega = [p, q, r]^T \in \mathbb{R}^3$ in the body-fixed frame $\mathcal{B}$, and m_s is the total mass of the vehicle. The Euler angles are expressed by roll ϕ, pitch θ, and yaw ψ. The moment of inertia is denoted by $J = diag(J_x, J_y, J_z) \in \mathbb{R}^{3\times3}$ defined in $\mathcal{B}$, τ expresses the moments in $\mathcal{B}$, $\hat{\Omega}$ introduces the skew-symmetric matrix of the vector Ω, R means the rotation matrix from $\mathcal{B}$ to $\mathcal{I}$, and F are the forces produced by the motors. By considering the previous assumptions and using the Newton–Euler formalism, (25) can be expressed as follows [29]:

$$\begin{aligned} \dot{p}_x &= v_x, \\ \dot{p}_y &= v_y, \\ \dot{p}_z &= v_z, \\ \dot{v}_x &= \big(\boldsymbol{c}\psi\boldsymbol{s}\theta\boldsymbol{c}\phi + \boldsymbol{s}\psi\boldsymbol{s}\phi\big)\frac{1}{m_s}u_z - \frac{d_f}{m_s}v_x, \\ \dot{v}_y &= \big(\boldsymbol{s}\psi\boldsymbol{s}\theta\boldsymbol{c}\phi - \boldsymbol{c}\psi\boldsymbol{s}\phi\big)\frac{1}{m_s}u_z - \frac{d_f}{m_s}v_y, \\ \dot{v}_z &= -g + \big(\boldsymbol{c}\theta\boldsymbol{c}\phi\big)\frac{1}{m_s}u_z - \frac{d_f}{m_s}v_z, \\ \dot{\phi} &= p + \big(\boldsymbol{s}\phi\boldsymbol{tan}\theta\big)q + \big(\boldsymbol{c}\phi\boldsymbol{tan}\theta\big)r, \\ \dot{\theta} &= \boldsymbol{c}\phi q - \boldsymbol{s}\phi r, \\ \dot{\psi} &= \big(\boldsymbol{s}\phi q + \boldsymbol{c}\phi r\big)\frac{1}{\boldsymbol{c}\theta}, \\ \dot{p} &= \big(qr(J_y - J_z) + u_\phi\big)\frac{1}{J_x} - \frac{d_t}{J_x}p, \\ \dot{q} &= \big(pr(J_z - J_x) + u_\theta\big)\frac{1}{J_y} - \frac{d_t}{J_y}q, \\ \dot{r} &= \big(pq(J_x - J_y) + u_\psi\big)\frac{1}{J_z} - \frac{d_t}{J_z}r, \end{aligned} \tag{26}$$

where $\boldsymbol{c}, \boldsymbol{s}$ and $\boldsymbol{tan}$ denote the trigonometric functions $\boldsymbol{cosine}, \boldsymbol{sine}$ and $\boldsymbol{tangent}$, respectively. The system inputs for the translational and attitude dynamics are defined as $u = [u_z, u_\phi, u_\theta, u_\psi]^T$. The real inputs of the system are the upward-lifting forces generated by each propeller, defined as f_1, f_2, f_3 and f_4 (see Fig. 1).

A. Model simplification

Some considerations are made for the full nonlinear system (26) in order to obtain a simpler model for control design purposes. When the vehicle is near to hover, the rotational dynamics can be simplified by considering that $(\dot{\phi}, \dot{\theta}, \dot{\psi}) \approx (p, q, r)$ [32]. Also, if the hover condition is established during the entire flight period $u_z \approx m_s g$. Drag force and drag torque can be considered null when the vehicle velocity is low. Therefore, the nonlinear equation for the quadcopter vehicle (26) is rewritten in an quasi-LPV state-space form as follows:

$$\begin{aligned} \dot{x} &= A(\zeta)x + B(\zeta)u, \\ y &= Cx, \end{aligned} \tag{27}$$

with

$$A(\zeta) = \begin{bmatrix} 0 & 1 & 0 & 0 & 0 & 0 & 0 & 0 & 0 & 0 & 0 & 0 \\ 0 & 0 & 0 & 0 & 0 & 0 & 0 & 0 & g & 0 & 0 & 0 \\ 0 & 0 & 0 & 1 & 0 & 0 & 0 & 0 & 0 & 0 & 0 & 0 \\ 0 & 0 & 0 & 0 & 0 & 0 & -g & 0 & 0 & 0 & 0 & 0 \\ 0 & 0 & 0 & 0 & 0 & 1 & 0 & 0 & 0 & 0 & 0 & 0 \\ 0 & 0 & 0 & 0 & 0 & 0 & 0 & 0 & 0 & 0 & 0 & 0 \\ 0 & 0 & 0 & 0 & 0 & 0 & 0 & 1 & 0 & 0 & 0 & 0 \\ 0 & 0 & 0 & 0 & 0 & 0 & 0 & 0 & 0 & 0 & 0 & Q_1\zeta_3 \\ 0 & 0 & 0 & 0 & 0 & 0 & 0 & 0 & 0 & 1 & 0 & 0 \\ 0 & 0 & 0 & 0 & 0 & 0 & 0 & 0 & 0 & 0 & 0 & Q_2\zeta_2 \\ 0 & 0 & 0 & 0 & 0 & 0 & 0 & 0 & 0 & 0 & 0 & 1 \\ 0 & 0 & 0 & 0 & 0 & 0 & 0 & Q_3\zeta_3 & 0 & 0 & 0 & 0 \end{bmatrix},$$

$$B(\zeta)=\begin{bmatrix} 0 & 0 & 0 & 0 \\ 0 & 0 & 0 & 0 \\ 0 & 0 & 0 & 0 \\ 0 & 0 & 0 & 0 \\ 0 & 0 & 0 & 0 \\ \zeta_1/m_s & 0 & 0 & 0 \\ 0 & 0 & 0 & 0 \\ 0 & 1/J_x & 0 & 0 \\ 0 & 0 & 0 & 0 \\ 0 & 0 & 1/J_y & 0 \\ 0 & 0 & 0 & 0 \\ 0 & 0 & 0 & 1/J_z \end{bmatrix},$$

where $\zeta_1 = \boldsymbol{c}\theta\boldsymbol{c}\phi$, $\zeta_2 = \dot{\phi}$, $\zeta_3 = \dot{\theta}$, $Q_1 = (J_y - J_z)/J_x$, $Q_2 = (J_z - J_x)/J_y$, and $Q_3 = (J_x - J_y)/J_z$. The state vector for one quadcopter vehicle is defined as $x = [p_x, v_x, p_y, v_y, p_z, v_z, \phi, \dot{\phi}, \theta, \dot{\theta}, \psi, \dot{\psi}]^T$ and C matrix is chosen in order that the output vector is $y = [p_x, p_y, p_z, \phi, \theta, \psi]$. The dynamic system (27) is modeled as a quasi-LPV representation in order to design an effective leader-following consensus.

B. Quasi-LPV representation

Based on the sector-nonlinearity technique [33], the number of local linear models is directly related to the number of nonlinear terms. For each nonlinear term, two sub-models are obtained such that for $\bar{f}$ nonlinear terms, the global model is composed of $m = 2^{\bar{f}}$ sub-models. The scheduling variables $\zeta = [\zeta_1, \zeta_2, \zeta_3]^T$ are the non-constant elements in (27), where $\zeta_1 \in [0.5, 1](\text{rad})$, $\zeta_2 \in [-\pi/2, \pi/2](\text{rad/s})$, and $\zeta_3 \in [-\pi/2, \pi/2](\text{rad/s})$, these constraints are acceptable when assuming slow dynamic reference displacements. The scheduling vector is defined as $\zeta \in [\zeta_f^0, \zeta_f^1]$; where ζ_f^0 and ζ_f^1 represents the minimum and maximum scalar values of ζ_f, respectively, with $f = 1, \ldots, 3$. For each scheduling variable, two weighting functions are computed as follows:

$$\mu_f^0 = \frac{\zeta_f^1 - \zeta_f}{\zeta_f^1 - \zeta_f^0}, \quad \mu_f^1 = 1 - \mu_f^0, \tag{28}$$

Thus, applying (28) to the quadcopter vehicle, the weighting functions are expressed as:

$$\begin{aligned} \mu_1^0 &= \frac{1 - \boldsymbol{c}\theta\boldsymbol{c}\phi}{0.5}, & \mu_1^1 &= 1 - \mu_1^0, \\ \mu_2^0 &= \frac{\pi - 2\dot{\phi}}{2\pi}, & \mu_2^1 &= 1 - \mu_2^0, \\ \mu_3^0 &= \frac{\pi - 2\dot{\theta}}{2\pi}, & \mu_3^1 &= 1 - \mu_3^0, \end{aligned} \tag{29}$$

Therefore, for $\bar{f} = 3$, $m = 8$ scheduling functions are computed as the product of the weighting functions that correspond to each local model, as:

$$\begin{aligned} \rho_1(\zeta) &= \mu_1^0\mu_2^0\mu_3^0, \quad \rho_2(\zeta) = \mu_1^0\mu_2^0\mu_3^1, \\ \rho_3(\zeta) &= \mu_1^0\mu_2^1\mu_3^0, \quad \rho_4(\zeta) = \mu_1^0\mu_2^1\mu_3^1, \\ \rho_5(\zeta) &= \mu_1^1\mu_2^0\mu_3^0, \quad \rho_6(\zeta) = \mu_1^1\mu_2^0\mu_3^1, \\ \rho_7(\zeta) &= \mu_1^1\mu_2^1\mu_3^0, \quad \rho_8(\zeta) = \mu_1^1\mu_2^1\mu_3^1, \end{aligned} \tag{30}$$

satisfying the convex set sum property in (4). Note that (30) can be rewritten, as $\rho_h(\zeta) = \mu_{h_1}^1\mu_{h_2}^2\mu_{h_3}^3$, where $[h_1, h_2, h_3]$ is the 3-digit binary representation of $(h-1)$. The known matrices A_h and B_h, with $h = 1, \ldots, 8$ (defining the 8 sub-models) are computed by replacing the scheduling variables ζ_f^0 or ζ_f^1, with $f = 1, 2$ and 3, to the matrices $A(\zeta)$ and $B(\zeta)$ in (27), such that:

$$A_h = A\big(\zeta_1^{h_1}, \zeta_2^{h_2}, \zeta_3^{h_3}\big), \qquad B_h = B\big(\zeta_1^{h_1}, \zeta_2^{h_2}, \zeta_3^{h_3}\big), \tag{31}$$

where ζ_f indicate which portion of the f–th scheduling variable is involved in the h–th sub-model. Consequently, by using the scheduling functions given by (30), the nonlinear system (27) is exactly represented as the following quasi-LPV model:

$$\begin{aligned} \dot{x} &= \sum_{h=1}^{8} \rho_h(\zeta)\big(A_h x + B_h u\big), \\ y &= Cx. \end{aligned} \tag{32}$$

V. SIMULATIONS RESULTS

In this section, the proposed leader-following consensus formation control based on MASs is applied to a fleet of five identical quadcopters. The two objectives of the MAS are to follow the trajectories described by a virtual leader and maintain a desired shape. The dynamic model of the virtual leader and followers is considered as (26), and the parameters of the UAVs are described in Table I.

TABLE I
PARAMETERS OF THE VTOL-UAV.

Parameter	Value	Unit
Mass of the vehicle, m_s	1.4	Kg
Acceleration due to gravity, g	9.81	m/s^2
Drag force coefficient, d_f	0.1	Ns
Drag torque coefficient, d_t	0.8	Nms
Moment of inertia about x, J_x	0.02	Kgm^2
Moment of inertia about y, J_y	0.03	Kgm^2
Moment of inertia about z, J_z	0.04	Kgm^2

The initial conditions of the quadcopters and their respective observers are presented in Table II.

TABLE II
INITIAL CONDITIONS.

Quadcopter	p_{x_i}	p_{y_i}	p_{z_i}	$\hat{p}_{x_i}$	$\hat{p}_{y_i}$	$\hat{p}_{z_i}$
1	6	-5	0	8	-3.5	0
2	3	-5	0	4	-7	0
3	0	-5	0	-1.5	-6	0
4	-3	-5	0	-4	-4	0
5	-6	-5	0	-8	-3	0

The initial conditions of the axis velocities, the angles, and the angular velocities are zero for all UAVs and observers. All the initial states of the virtual leader are zero.

To solve the formation control consensus-based problem the control law (7) is considered as:

$$u_i = K_h \left[\sum_{j \in \mathcal{N}_i} a_{ij}(\hat{\bar{s}}_i - \hat{\bar{s}}_j) + \alpha_i(\hat{\bar{s}}_i - \bar{s}_l) \right], \tag{33}$$

where $\hat{\bar{s}}_i(t) = [\hat{p}_i^T - h_i^T, \hat{v}_i^T, \hat{\omega}_i^T, \hat{\dot{\omega}}_i^T]^T$, is the estimated state vector of agent i and $\bar{s}_l = [p_l^T, v_l^T, \omega_l^T, \dot{\omega}_l^T]^T$ is the virtual leader state vector. Considering $p_i = [p_{xi}, p_{yi}, p_{zi}]$, $v_i = [v_{xi}, v_{yi}, v_{zi}]$, $\omega = [\phi_i, \theta_i, \psi_i]$, $\dot{\omega} = [\dot{\phi}_i, \dot{\theta}_i, \dot{\psi}_i]$, and u_i the position, the axis velocities, the angular position, the angular velocities, and the acceleration respectively of agent i, $H = [h_1^T, h_2^T, \ldots, h_N^T]^T$ contains the desired distance column vectors h_i of every agent. In this example, the following matrix H is used to perform the formation of a pentagon:

$$H = r \cdot \begin{bmatrix} \boldsymbol{s}(36) & \boldsymbol{s}(108) & \boldsymbol{s}(180) & \boldsymbol{s}(252) & \boldsymbol{s}(324) \\ -\boldsymbol{c}(36) & -\boldsymbol{c}(108) & -\boldsymbol{c}(180) & -\boldsymbol{c}(252) & -\boldsymbol{c}(324) \\ 0 & 0 & 0 & 0 & 0 \end{bmatrix} \quad (34)$$

where $r = 4$ is the radius of the pentagon and the distance between the leader and each UAV. The communication topology is illustrated in Fig. 2.

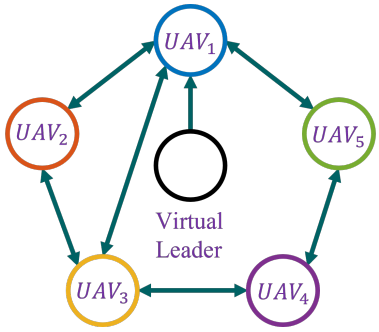

Fig. 2. Communication links between UAVs.

Based on Fig. 2, the communication with the virtual leader is denoted by $\Lambda = diag(1, 0, 0, 0, 0)$ and the Laplacian matrix:

$$\mathcal{L} = \begin{bmatrix} 3 & -1 & -1 & 0 & -1 \\ -1 & 2 & -1 & 0 & 0 \\ -1 & -1 & 3 & -1 & 0 \\ 0 & 0 & -1 & 2 & -1 \\ -1 & 0 & 0 & -1 & 2 \end{bmatrix}. \quad (35)$$

To compute the vertex control gains K_h and the vertex observer gains L_h, the quasi-LPV representation of the UAVs (27) is used to find a solution for the LMIs presented in Theorem 1 with $\mu = 0.001$ using Matlab software with the toolbox SDPT3 [34].

To prove the performance of the LPV observer (8), the estimation error $e_i = y_i - \hat{y}_i$ is shown in Fig. 3, where the convergence of all the estimated states of all agents is guaranteed. Sensor noise was added as a random function with normal distribution, a mean value of zero, and a standard deviation of 0.003.

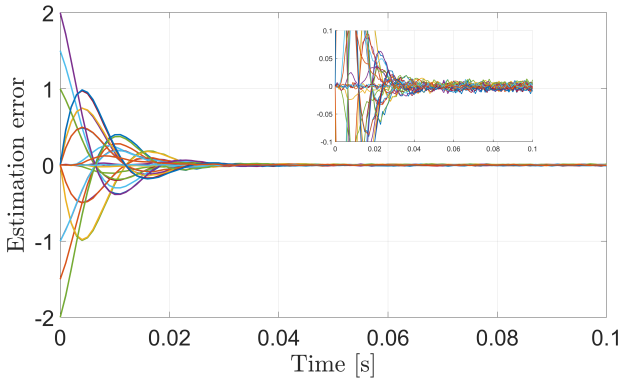

Fig. 3. Observer convergence.

The objective of the virtual leader is to be the center of the pentagon and reach the reference position $[0, 0, 20]^T$ which corresponds with the axis p_x, p_y, and p_z. In order to track a smooth trajectory, the following trajectory planning (36) is used as a change of reference for the altitude of the virtual leader:

$$\begin{aligned} z_{ref}(t) =& z(0) + (10/T^3)[z(T) - z(0)]t^3 - \\ & (15/T^4)[z(T) - z(0)]t^4 + (6/T^5)[z(T) - z(0)]t^5. \end{aligned} \quad (36)$$

where $z(0) = 0$ is the initial position of the virtual leader, $z(T) = 20\text{m}$ is the desired altitude, $T = 5\text{s}$ is the period of time between $z(0)$ and $z(T)$. To synthesize (36) the initial and final conditions of the velocity $\dot{z}_{ref}$ and the acceleration $\ddot{z}_{ref}$ are considered as zero to ensure a smooth trajectory. Fig. 4 shows the trajectory reference z_{ref}, the virtual leader z_l, and all UAVs altitudes z_i.

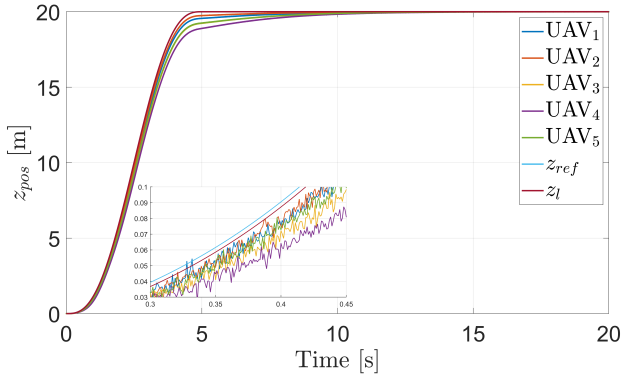

Fig. 4. Trajectory planning of the virtual leader in z-axis.

If the altitude reference is a step of 20m, an overshoot occurs in the thrust u_z outside the physical limitations allowable by a UAV, the overshoot is removed with the trajectory planning (36) and all the obtained thrust in Fig. 5 are at appropriate physical values. Fig. 5 shows the obtained thrust u_z for the virtual leader and the five quadcopters when (36) is considered for the virtual leader.

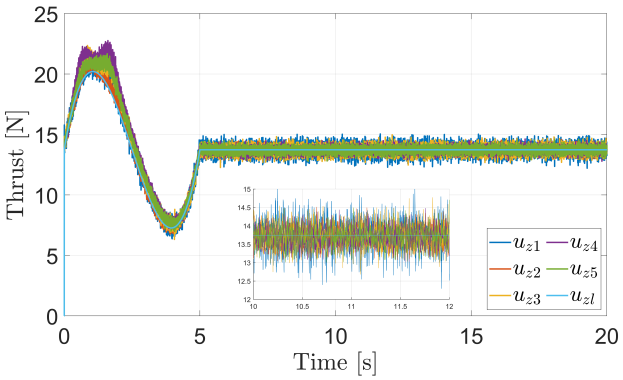

Fig. 5. Thrust of the leader and the followers.

Fig. 6 shows the performance of the quadcopters' trajectories. The leader quadcopter is in the middle of all the followers in black color at the desired altitude. The followers reach their desired position in the vertex of the pentagon highlighted in green color.

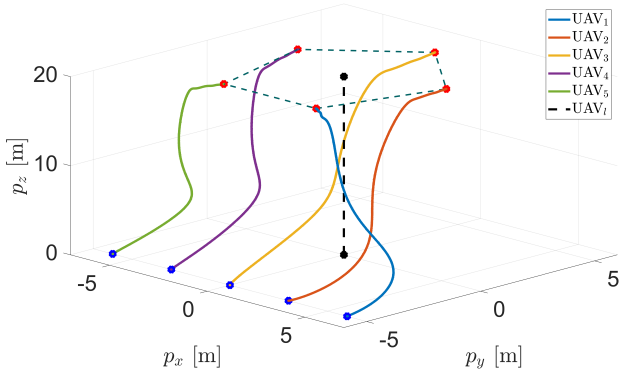

Fig. 6. Trajectories of the quadcopters.

To measure the synchronization error in this example, let us define $\delta_i = \|x_i - x_l\| - r$. Fig. 7 represents the evolution of δ_i. The quadcopters follow the leader's trajectories in their desired pentagon vertex when $\delta_i = 0$.

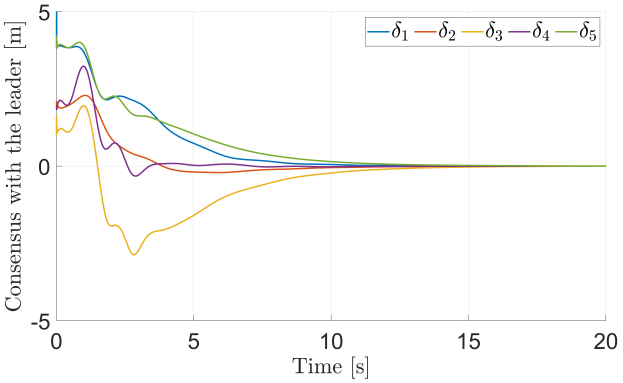

Fig. 7. Synchronization error.

Let us define $d_{ij} = \|([x_i, y_i, z_i]^T - [x_j, y_j, z_j]^T) - (h_i - h_j)\|$ if $d_{ij} = 0$, then, the desired formation is reached. Fig. 8 illustrates the relative distances performance between the quadcopters to reach the desired formation H.

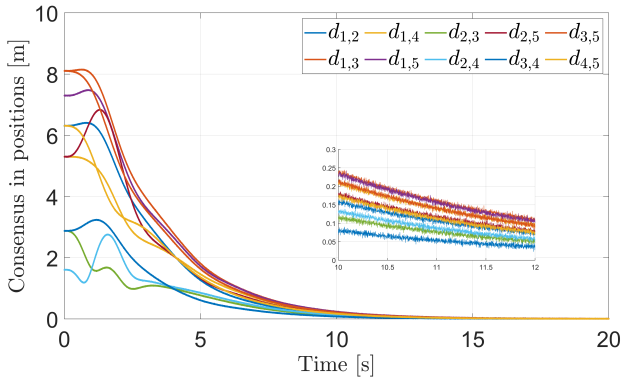

Fig. 8. Distances between followers to reach the formation.

VI. CONCLUSIONS

A distributed leader-following consensus control for LPV multi-agent systems was presented. The LMIs conditions to compute the control and observer gains were presented considering the less conservative Polya's theorem. The simulation results show that a team of UAVs was able to follow the trajectories of a virtual leader and maintain a desired formation with the proposed approach. As an extension of this work, collision avoidance and communication constraint management are suggested. Because an agent can be affected by actuator or sensor faults, compromising the global objective of the team, an LMI-based fault-tolerant control for LPV multi-agent systems is proposed for future work.

REFERENCES

[1] Ziquan YU, Youmin ZHANG, Bin JIANG, Jun FU, and Ying JIN. A review on fault-tolerant cooperative control of multiple unmanned aerial vehicles. *Chinese Journal of Aeronautics*, 35(1):1–18, 2022.

[2] Zhongkui Li and Duan Zhisheng. *Cooperative Control of Multi-Agent Systems: A Consensus Region Approach*. CRC Press, 2017.

[3] Muhammad Rehan, Choon Ki Ahn, and Mohammed Chadli. Consensus of one-sided lipschitz multi-agents under input saturation. *IEEE Transactions on Circuits and Systems II: Express Briefs*, 67(4):745–749, 2020.

[4] Minhong He, Jingru Mu, and Xiaowu Mu. h_∞ leader-following consensus of nonlinear multi-agent systems under semi-markovian switching topologies with partially unknown transition rates. *Information Sciences*, 513:168–179, 2020.

[5] Xun Yan, Dapeng Jiang, Runlong Miao, and Yulong Li. Formation control and obstacle avoidance algorithm of a multi-usv system based on virtual structure and artificial potential field. *Journal of Marine Science and Engineering*, 9(2), 2021.

[6] Jie Huang et al. Distributed behavioral control for second-order nonlinear multi-agent systems. *IFAC-PapersOnLine*, 50(1):2445–2450, 2017. 20th IFAC World Congress.

[7] Xiaomei Liu, Shuzhi Sam Ge, and Cher-Hiang Goh. Formation potential field for trajectory tracking control of multi-agents in constrained space. *International Journal of Control*, 90(10):2137–2151, 2017.

[8] Dongyu Li, Shuzhi Sam Ge, Wei He, Guangfu Ma, and Lihua Xie. Multilayer formation control of multi-agent systems. *Automatica*, 109:108558, 2019.

[9] Zhi Yan, Nicolas Jouandeau, and Arab Ali Cherif. A survey and analysis of multi-robot coordination. *International Journal of Advanced Robotic Systems*, 10(12):399, 2013.

[10] Jesus A. Vazquez Trejo, Jean-Christophe Ponsart, Manuel Adam-Medina, Guillermo Valencia-Palomo, and Juan Antonio Vazquez Trejo. Distributed observer-based leader-following consensus control robust to external disturbance and measurement sensor noise for lti multi-agent systems. In *16th European Workshop on Advanced Control and Diagnosis, ACD 2022*, 2022.

[11] Xiwang Dong, Yan Zhou, Zhang Ren, and Yisheng Zhong. Time-varying formation tracking for second-order multi-agent systems subjected to switching topologies with application to quadrotor formation flying. *IEEE Transactions on Industrial Electronics*, 64(6):5014–5024, 2017.

[12] Adeel Zaidi, Muhammad Kazim, Rui Weng, Dongzhe Wang, and Xu Zhang. Distributed observer-based leader following consensus tracking protocol for a swarm of drones. *Journal of Intelligent & Robotic Systems*, 102(3):64, 2021.

[13] Taha Elmokadem. Distributed coverage control of quadrotor multi-uav systems for precision agriculture. *IFAC-PapersOnLine*, 52(30):251–256, 2019. 6th IFAC Conference on Sensing, Control and Automation Technologies for Agriculture AGRICONTROL 2019.

[14] David Paez et al. Distributed particle swarm optimization for multi-robot system in search and rescue operations. *IFAC-PapersOnLine*, 54(4):1–6, 2021. 4th IFAC Conference on Embedded Systems, Computational Intelligence and Telematics in Control CESCIT 2021.

[15] Guangcheng Wang et al. A multi-auv maritime target search method for moving and invisible objects based on multi-agent deep reinforcement learning. *Sensors*, 22(21), 2022.

[16] Junyan Hu et al. Fault-tolerant cooperative navigation of networked uav swarms for forest fire monitoring. *Aerospace Science and Technology*, 123:107494, 2022.

[17] Moad Idrissi, Mohammad Salami, and Fawaz Annaz. A review of quadrotor unmanned aerial vehicles: Applications, architectural design and control algorithms. *Journal of Intelligent & Robotic Systems*, 104(2):1–33, 2022.

[18] Jianhua Wang et al. Time-varying formation of second-order discrete-time multi-agent systems under non-uniform communication delays and switching topology with application to uav formation flying. *IET Control Theory & Applications*, 14(14):1947–1956, 2020.

[19] Adel Belkadi, Laurent Ciarletta, and Didier Theilliol. Particle swarm optimization method for the control of a fleet of unmanned aerial vehicles. *Journal of Physics: Conference Series*, 659:012015, 2015.

[20] Juan Antonio Vazquez Trejo, Damiano Rotondo, Manuel Adam-Medina, and Didier Theilliol. Observer-based event-triggered model reference control for multi-agent systems. In *2020 International Conference on Unmanned Aircraft Systems (ICUAS)*, pages 421–428, 2020.

[21] Juan Antonio Vazquez Trejo, Didier Theilliol, Manuel Adam Medina, C. D. García Beltrán, and Marcin Witczak. Leader-following formation control for networked multi-agent systems under communication faults/failures. In *Advances in Diagnostics of Processes and Systems*, pages 45–57. Springer International Publishing, Cham, 2021.

[22] Jianliang Chen, Weidong Zhang, Yong-Yan Cao, and Hongjun Chu. Observer-based consensus control against actuator faults for linear parameter-varying multiagent systems. *IEEE Transactions on Systems, Man, and Cybernetics: Systems*, 47(7):1336–1347, 2017.

[23] Damiano Rotondo, Jean-Christophe Ponsart, and Didier Theilliol. Gain-scheduled observer-based consensus for linear parameter varying multi-agent systems. *Automatica*, 135:109979, 2022.

[24] Antonio Sala and Carlos Ariño. Asymptotically necessary and sufficient conditions for stability and performance in fuzzy control: Applications of polya's theorem. *Fuzzy Sets and Systems*, 158(24):2671–2686, 2007. Theme: Modelling and Control.

[25] Kemin Zhou and John Comstock Doyle. *Essentials of robust control*, volume 104. Prentice-Hall, 1998.

[26] Stephen Boyd, Laurent El Ghaoui, Eric Feron, and Venkataramanan Balakrishnan. *Linear matrix inequalities in system and control theory*. SIAM, 1994.

[27] X.-D. Sun and I. Postlethwaite. Affine lpv modelling and its use in gain-scheduled helicopter control. In *UKACC International Conference on Control '98 (Conf. Publ. No. 455)*, pages 1504–1509 vol.2, 1998.

[28] Damiano Rotondo, Helem Sánchez, Fatiha Nejjari, and Vicenç Puig. Analysis and design of linear parameter varying systems using lmis. *Revista Iberoamericana de Automatica e Informatica Industrial (RIAI)*, 16, 11 2018.

[29] Iman Sadeghzadeh, Abbas Chamseddine, Didier Theilliol, and Youmin Zhang. Linear parameter varying control synthesis: State feedback versus h_∞ technique with application to quadrotor ua v. In *2014 International Conference on Unmanned Aircraft Systems (ICUAS)*, pages 1099–1104, 2014.

[30] Gerardo Ortiz-Torres et al. Fault estimation and fault tolerant control strategies applied to vtol aerial vehicles with soft and aggressive actuator faults. *IEEE Access*, 8:10649–10661, 2020.

[31] G. Ortiz-Torres, P. Castillo, and J. Reyes-Reyes. An actuator fault tolerant control for vtol vehicles using fault estimation observers: Practical validation. In *2018 International Conference on Unmanned Aircraft Systems (ICUAS)*, pages 1054–1062, 2018.

[32] Hammad Zaki, Mustafa Unel, and Yildiray Yildiz. Trajectory control of a quadrotor using a control allocation approach. In *2017 International Conference on Unmanned Aircraft Systems (ICUAS)*, pages 533–539, 2017.

[33] Hiroshi Ohtake, Kazuo Tanaka, and Hua O Wang. Fuzzy modeling via sector nonlinearity concept. *Integrated Computer-Aided Engineering*, 10(4):333–341, 2003.

[34] Kim-Chuan Toh, Michael J Todd, and Reha H Tütüncü. Sdpt3—a matlab software package for semidefinite programming, version 1.3. *Optimization methods and software*, 11(1-4):545–581, 1999.